Received: 26 June 2023 | Revised: 29 November 2023 | Accepted: 4 December 2023

DOI: 10.1111/cas.16047

Cancer Science WILEY

ORIGINAL ARTICLE

Tumor suppressive function of IGF2BP1 in gastric cancer through decreasing MYC

Ning Ding[1,2,3] | Guodong Cao[4] | Zhuo Wang[1,2,3] | Shengjun Xu[5,6] | Wenwen Chen[1,2,3]

[1]Department of Gastroenterology, The Second Affiliated Hospital of Zhejiang University School of Medicine, Hangzhou, China

[2]Zhejiang University Cancer Center, Hangzhou, China

[3]Institution of Gastroenterology, Zhejiang University, Hangzhou, China

[4]Department of General Surgery, First Affiliated Hospital of Anhui Medical University, Hefei, China

[5]Key Laboratory of Integrated Oncology and Intelligent Medicine of Zhejiang Province, Hangzhou, China

[6]Department of Hepatobiliary and Pancreatic Surgery, Hangzhou First People's Hospital, Hangzhou, China

Correspondence
Wenwen Chen, Department of Gastroenterology, the Second Affiliated Hospital of Zhejiang University School of Medicine, No. 88 Jiefang Road, Hangzhou, Zhejiang 310009, China.
Email: 2520125@zju.edu.cn

Shengjun Xu, Key Laboratory of Integrated Oncology and Intelligent Medicine of Zhejiang Province, No. 261 Huansha Road, Hangzhou, Zhejiang 310006, China.
Email: zjuxsj@zju.edu.cn

Funding information
China Postdoctoral Science Foundation, Grant/Award Number: 2022M722764; Natural Science Foundation of Zhejiang Province, Grant/Award Number: LQ22C070003

Abstract

Gastric cancer is one of the most common causes of cancer-related death worldwide. The N^6-methyladenosine (m^6A) reader IGF2BP1 (insulin-like growth factor-2 mRNA binding protein 1) has been reported to promote cancer progression by stabilizing oncogenic mRNAs through its m^6A-binding activity in some tumors. However, the role of IGF2BP1 in gastric carcinogenesis remains unclear. In this study, we found that IGF2BP1 is significantly downregulated in tumor tissues from patients with gastric cancer. Lower expression of IGF2BP1 is associated with poor prognosis. Gastric cancer cell proliferation is suppressed by IGF2BP1 in an m^6A-dependent manner. Additionally, IGF2BP1 is able to significantly attenuate tumor growth of gastric cancer cells. Further m^6A sequencing and m^6A-RNA immunoprecipitation assays show that *MYC* (c-myc proto-oncogene) mRNA is a target transcript of IGF2BP1 in gastric cancer cells. IGF2BP1 inhibits gastric cancer cell proliferation by reducing the mRNA and protein expression of MYC. Mechanistically, IGF2BP1 promotes the degradation of *MYC* mRNA and inhibits its translation efficiency. Taken together, these data suggest that IGF2BP1 plays a tumor-suppressive role in gastric carcinogenesis by downregulating MYC in an m^6A-dependent manner, thereby making the IGF2BP1-*MYC* axis a potential target for gastric cancer treatment.

KEYWORDS
gastric cancer, IGF2BP1, m^6A, MYC, RNA metabolism

Abbreviations: IGF2BP1, insulin-like growth factor-2 mRNA binding protein 1; KH, type-I hnRNP K homology; lgFDR, $\log_{10}$(false discovery rate); m^6A, N^6-methyladenosine; MYC, c-myc proto-oncogene; qPCR, quantitative PCR; RBM15B, RNA binding motif protein 15B; RIP, RNA immunoprecipitation; seq, sequencing.

1 | INTRODUCTION

Gastric cancer was responsible for over 1 million new cases and an estimated 769,000 deaths in 2020, ranking fifth for incidence and fourth for mortality globally.[1] Therefore, it is important to understand the molecular mechanism of gastric cancer progression, which is of great significance for its early diagnosis and precision treatment.

N^6-methyladenosine RNA modification is one of the most abundant internal modifications in eukaryotic mRNAs.[2] The highly dynamic and reversible m^6A modification of mRNAs is mediated by proteins that install, recognize, and remove m^6A sites. The writer complex of m^6A consists of a methyltransferase-like 3 catalytic subunit and other accessory subunits,[3,4] while FTO alpha-ketoglutarate dependent dioxygenase or alkB homolog 5 constitutes the demethylases (erasers).[5,6] N^6-methyladenosine RNA-binding proteins (readers) can specifically recognize and bind to m^6A-modified mRNAs, thereby regulating the metabolism of methylated mRNAs.[7–9] As m^6A modification of mRNAs is involved in the regulation of nearly every aspect of the mRNA life cycle, including splicing, transport, stability, and translation, it plays crucial roles in various developmental processes and human cancers.[4,10] However, the role of m^6A modification in gastric cancer remains elusive.

Insulin-like growth factor 2 mRNA-binding proteins (including IGF2BP1–3) have been reported as a distinct family of m^6A readers.[11] The IGF2BPs contain six characteristic RNA-binding domains, including four type I hnRNP KH domains at the C-terminus and two RNA recognition motifs at the N-terminal end.[12] KH domains, particularly KH3 and KH4 domains, are essential for the binding and recognition of the consensus GG (m^6A) C sequence of m^6A-modified mRNAs.[11] The IGF2BP family has been documented to have important functions in many biological processes, such as embryo development and cancer progression, by regulating RNA metabolism processes.[13] Recent studies show that IGF2BP1 plays the most conserved oncogenic role among all members of the IGF2BP family in tumor-derived cells[14,15]; nevertheless, the regulatory mechanism of IGF2BP1 in gastric cancer is still unclear.

Here, we found that IGF2BP1 is significantly reduced in tumor tissues from patients with gastric cancer, which is also correlated with shorter survival times. Additionally, IGF2BP1 suppresses gastric cancer cell proliferation in an m^6A-dependent manner along with inhibition of the tumor growth of gastric cancer cells. IGF2BP1 has been show to not only promote *MYC* mRNA degradation, but also inhibit its translation efficiency. Collectively, our data suggest that the m^6A reader *IGF2BP1* functions as a tumor-suppressive gene in gastric cancer development.

2 | MATERIALS AND METHODS

2.1 | Samples

Primary gastric cancer and paracancerous gastric mucosa tissues were obtained from three cohorts of patients with gastric cancer. The use of clinical samples was approved by the Ethics Committee of the Second Affiliated Hospital of Zhejiang University School of Medicine (2022–0927).

2.2 | Cell culture and transfection

The gastric cancer cell line MKN45 and GES-1 was obtained from the Chinese Academy of Medical Sciences. AGS, HGC, MGC, N87 and HEK-293T cells were obtained from the Cell Bank of the Chinese Academy of Sciences. SGC cells were obtained from Beijing Cancer Hospital. BGC cells were obtained from the Chinese Academy of Sciences. WP6 cells were obtained from The First Affiliated Hospital of Zhejiang University School of Medicine. MKN45, AGS, HGC, MGC, N87, SGC, BGC, and WP6 cells were cultured in RPMI-1640 medium supplemented with 10% FBS and 1% antibiotics. GES-1 and HEK-239T cells were maintained in DMEM supplemented with 10% FBS and 1% antibiotics. All the cell lines were maintained at 37°C in a humidified atmosphere containing 5% CO_2. Plasmids and siRNAs were transfected into cells using PolyJet (SignaGen) or Lipofectamine RNAiMAX (Invitrogen), according to the manufacturer's instructions.

2.3 | Plasmids

Full-length IGF2BP1 was amplified from first-strand cDNA and cloned into pLVX-Puro vectors; pLVX-IGF2BP1 forward primer, 5′-GTCAGAATTCATGAACAAGCTTTACATCGG-3′ and reverse primer, 5′-GTCAGGATCCTCACTTCCTCCGTGCCTGGG-3′. The IGF2BP1-KH3/4 and IGF2BP1-KH1–4 plasmids were constructed with mutants of GxxG to GEEG in KH3 and KH4 domains or in KH1–4 domains on the basis of the WT plasmid. Empty pLVX-Puro vectors were transfected into cells and served as a control for overexpression assays.

2.4 | shRNAs and siRNAs

For transient knockdown, control siRNA, and siRNAs targeting IGF2BP1, MYC, and RBM15B were purchased from Tsingke Biotechnology. Their sequences were as follows: control siRNA, 5′-UUCUCCGAACGUGUCACGUTT-3′; IGF2BP1-siRNA1, 5′-CAAGGAAAACGCUUAGAGATT-3′ and IGF2BP1-siRNA2 5′-CCUAUAGCUCCUUUAUGCATT-3′; MYC-siRNA1 5′-CGAUGUUGUUUCUGUGGAATT-3′ and MYC-siRNA2 5′-CCAAGGUAGUUAUCCUUAATT-3′; RBM15B-siRNA1 5 ′-GCCUAUAUUCAGUACGAGA-3′ and RBM15B-siRNA2 5′-GCAACCUCUUCAUUGGUAA-3′.

For stable knockdown of IGF2BP1, oligos were cloned into the pLKO.1 vector. The shRNA sequences were as follows: IGF2BP1-shRNA1 5′-ACGCTTAGAGATTGAACATTC-3′ and IGF2BP1-shRNA2 5′-CTCCAAAGTTCGTATGGTTAT-3′. Lentiviruses were packaged with the pLKO.1, pCMV-8.91, and VSV-G plasmids in HEK-239T cells. MKN45 cells were infected with the lentivirus-containing medium for

48 h and then selected using puromycin. Empty pLKO.1 vectors were packaged into lentiviruses and served as a control for stable knockdown assays. For rescue experiments, IGF2BP1 and IGF2BP1-KH1-4 mutant plasmids were produced with synonymous mutants in the target sequences of siRNAs and shRNAs using PCR and cloned into pLVX-Puro vectors.

2.5 | RNA isolation, reverse transcription, and qPCR

Total RNA was isolated from cells or tissues using TRIzol reagent (Invitrogen) according to the manufacturer's instructions. cDNA was synthesized by reverse transcription of 1000 ng RNA using HiScript II Q RT SuperMix (Vazyme). Quantitative PCR was undertaken using ChamQ Universal SYBR qPCR Master Mix (Vazyme) in a LightCycler 480 II system (Roche). All reactions were carried out in triplicate. The mRNA expression was normalized to *GAPDH*. The primers used in qPCR assays are listed in Table S1.

2.6 | Western blot analysis

Cells or tissues were lysed using TBSN buffer (20 mM Tris, pH 8.0, 150 mM NaCl, 0.5% NP-40, 5 mM EGTA, 1.5 mM EDTA, 0.5 mM Na_3VO_4, 20 mM p-nitrophenyl phosphate) with protease inhibitor (Beyotime) on ice for 30 min. Equal amounts of protein were loaded and separated by 10% SDS-PAGE and then transferred to PVDF membranes (Millipore). The membranes were blocked with 5% nonfat milk in TBST buffer (20 mM Tris, pH 7.6, 137 mM NaCl, 0.1% Tween-20) for 1 h at room temperature, washed, and incubated with the indicated primary Abs overnight at 4°C. After washing with TBST, membranes were incubated with HRP-conjugated secondary Abs for 1 h at room temperature. The protein bands were detected using Clarity Western ECL Substrate (Bio-Rad) and the ChemiDoc Touch Imaging System (Bio-Rad). The Abs used for western blotting were as follows: IGF2BP1 (rabbit, 1:1000; Cell Signaling Technology, 8482), MYC (rabbit, 1:4000; Proteintech, 10,828-1-AP), and GAPDH (mouse, 1:10000; Proteintech, 60,004-1-Ig). The gray levels of all western blots were quantified. The relative expression levels were calculated by dividing the gray value of the target protein by the loading control (GAPDH).

2.7 | Immunohistochemistry

Gastric cancer tissue array was subjected to immunohistochemical staining with the same anti-IGF2BP1 Ab used in western blotting in accordance with a previously reported protocol with minor modifications.[16] The IGF2BP1 expression level was determined by immunohistochemistry scoring according to positive rate and staining intensity.

2.8 | Mouse studies

For the tumor xenograft model, 1×10^7 gastric cancer cells were injected s.c. into 4- to 6-week-old female BALB/C nude mice (Vitalriver). The mice were maintained in specific pathogen-free facilities. The mouse studies were approved by the Ethics Committee of the Second Affiliated Hospital of the Zhejiang University School of Medicine (2022–201). All institutional and national guidelines for the care and use of laboratory animals were followed.

2.9 | N^6-methyladenosine RIP seq

The m^6A-RIP seq was carried out in accordance with a previously reported protocol, with minor modifications.[17] Briefly, 2 μg of polyadenylated RNA was extracted using the NEBNext Poly(A) mRNA Magnetic Isolation Module (New England Biolabs) and then fragmented into ~150 nt fragments using magnesium RNA fragmentation buffer (New England Biolabs). Fragmented polyadenylated RNA (5%) was used as the input sample, and the remaining samples were diluted and incubated with 5 μg of anti-m^6A Ab (Synaptic Systems; 202,003) in IPP buffer (10 mM Tris, pH 7.4, 150 mM NaCl, 0.1% NP-40) supplemented with RiboLock RNase Inhibitor (Invitrogen) at 4°C with overnight shaking. The m^6A containing fragments were pulled down using Protein A/G PLUS-Agarose (Santa Cruz Biotechnology) and reverse transcribed to cDNA using SuperScript II (Invitrogen). Library construction was undertaken using the NEBNext Ultra II Non-Directional RNA Second Strand Synthesis Module and NEBNext Ultra II DNA Library Prep Kit for Illumina (New England Biolabs) according to the manufacturer's instructions. The samples were sequenced on an Illumina NovaSeq 6000 platform. The m^6A-seq data have been deposited into the GEO database under the accession number GSE243617.

2.10 | RNA sequencing

MKN45 cells were transfected with control or IGF2BP1 siRNA for 48 h in 1640 medium with 10% serum. Total RNA was extracted from control and IGF2BP1-depleted cells and subjected to library construction and sequencing (Novagene Company). The RNA-seq data have been deposited into the GEO database under the accession number GSE243617.

2.11 | RNA immunoprecipitation-qPCR

Cells were lysed using RIP buffer (25 mM Tris, pH 7.4, 150 mM KCl, 0.5 mM DTT, 0.5% NP-40). IGF2BP1 Abs (2 μg) or the corresponding IgG (Beyotime; A7016) were added to the lysis buffer and incubated for 12 h at 4°C. Protein A/G magnetic beads were then added to the lysis buffer and incubated for 4 h at 4°C, followed by washing three times with NT2 buffer (50 mM Tris, pH 7.4, 150 mM

NaCl, 1 mM $MgCl_2$, 0.05% NP-40). Input and immunoprecipitated RNAs were extracted using TRIzol reagent, followed by qRT-PCR.

2.12 | N^6-methyladenosine-RIP-qPCR

The m^6A modifications of individual genes were determined using the m^6A-RIP-qPCR assay. Briefly, 40 μg RNA was extracted from cells using TRIzol reagent and incubated with 1 μg anti-m^6A Ab or corresponding IgG in IPP buffer supplemented with RNase inhibitors at 4°C overnight with shaking. The mixture was then incubated with prewashed Protein A/G PLUS-Agarose for 4 h at 4°C with rotation. After washing three times with IPP buffer, m^6A containing RNAs was extracted using TRIzol reagent and reverse transcribed to cDNA. The same amount of original RNA was reverse-transcribed as input. Further enrichment was quantified using qPCR, and the corresponding m^6A enrichment of specific genes in each sample was calculated by normalizing to the input.

2.13 | RNA decay assay

MKN45 cells treated with IGF2BP1 siRNA or the corresponding control siRNA for 48 h were seeded into 12-well plates. The cells were then treated with 5 μg/mL actinomycin D (MedChemExpress) to suppress global RNA transcription after 48 h and were collected at different time points. Total RNA was extracted using TRIzol reagent and reverse transcribed into cDNA, followed by detection of *MYC* mRNA expression by qPCR.

2.14 | Polysome profiling

Polysome profiling was carried out as previously described.[18] Briefly, stable cells were treated with 10 μg/mL cycloheximide (MedChemExpress) for 5 min at 37°C. Then the cells were harvested, and 500 μL cytoplasmic extract was layered onto 11 mL of 5%–50% sucrose gradient and centrifuged at 36,000 rpm in a Beckman SW-41Ti rotor for 2.5 h at 4°C. The gradients were fractionated and monitored at an absorbance of 254 nm (Bruker). Polysome-associated and cytosolic RNA were isolated using TRIzol (Invitrogen) and analyzed by qPCR.

2.15 | Cell proliferation assays

MKN45 and AGS cells were seeded in 96-well plates at 3000–5000 cells per well. Cell viability was evaluated in the following 5 days at the same time using the CCK-8 assay (MedChemExpress). For the 2D colony formation assay, 500–1000 gastric cancer cells were seeded in 6-well plates for 5-7 days and stained with crystal violet later for counting the number of clones. For the 3D colony formation assay, 96-well plates were first seeded with 10 μL Matrigel Matrix (Corning). Following this, 3000–5000 gastric cancer cells dispersed in 50 μL culture medium were mixed thoroughly with 50 μL Matrigel Matrix and seeded in 96-well plates. Culture medium (50 μL) was then added to 96-well plates. After 7–10 days, colony size and number were counted using a microscope.

2.16 | Statistical analysis

Data are representative of at least three independent experiments. Unpaired two-tailed Student's *t*-test was applied to analyze the statistical significance between two groups, $p < 0.05$ was considered statistically significant. Statistical significance was defined as $^*p < 0.05$, $^{**}p < 0.01$, and $^{***}p < 0.001$.

3 | RESULTS

3.1 | Downregulation of IGF2BP1 in gastric cancer tissues is associated with reduced survival times in patients

To explore the role of IGF2BP1 in gastric cancer, we first examined the mRNA levels of IGF2BP1 in human gastric cancer tissues. Quantitative RT-PCR showed that the mRNA expression of *IGF2BP1* was significantly decreased in gastric cancer tissues compared to their matched nontumor tissues in cohort 1 ($n = 201$) (Figure 1A,B). Western blot analysis revealed that the protein levels of IGF2BP1 were also significantly downregulated in gastric cancer tissues versus nontumor tissues in cohort 2 ($n = 105$) (Figure 1C–E). Moreover, tissue microarray analysis confirmed that the protein expression of IGF2BP1 was significantly reduced in gastric cancer tissues in comparison to their paired nontumor tissues in cohort 3 ($n = 82$) (Figure 1F–H).

To determine the correlation between IGF2BP1 expression and clinical outcome, we undertook Kaplan–Meier analysis and found that low IGF2BP1 expression was significantly correlated with reduced overall survival time in patients with gastric cancer (Figure 1I). Further analysis of clinicopathologic features showed that lower expression of IGF2BP1 was significantly associated with poor differentiation, lymph node metastasis, and advanced TNM stages of gastric cancer (Table S2). Taken together, these data suggest that *IGF2BP1* could be a tumor-suppressive gene in gastric cancer.

3.2 | IGF2BP1 suppresses proliferation of gastric cancer cells

To investigate the function of IGF2BP1 in gastric cancer progression, we examined the expression levels of IGF2BP1 in various gastric cancer cell lines (Figure 2A). Western blot analysis revealed that IGF2BP1 was expressed at high levels in MKN45 cells, while the expression was

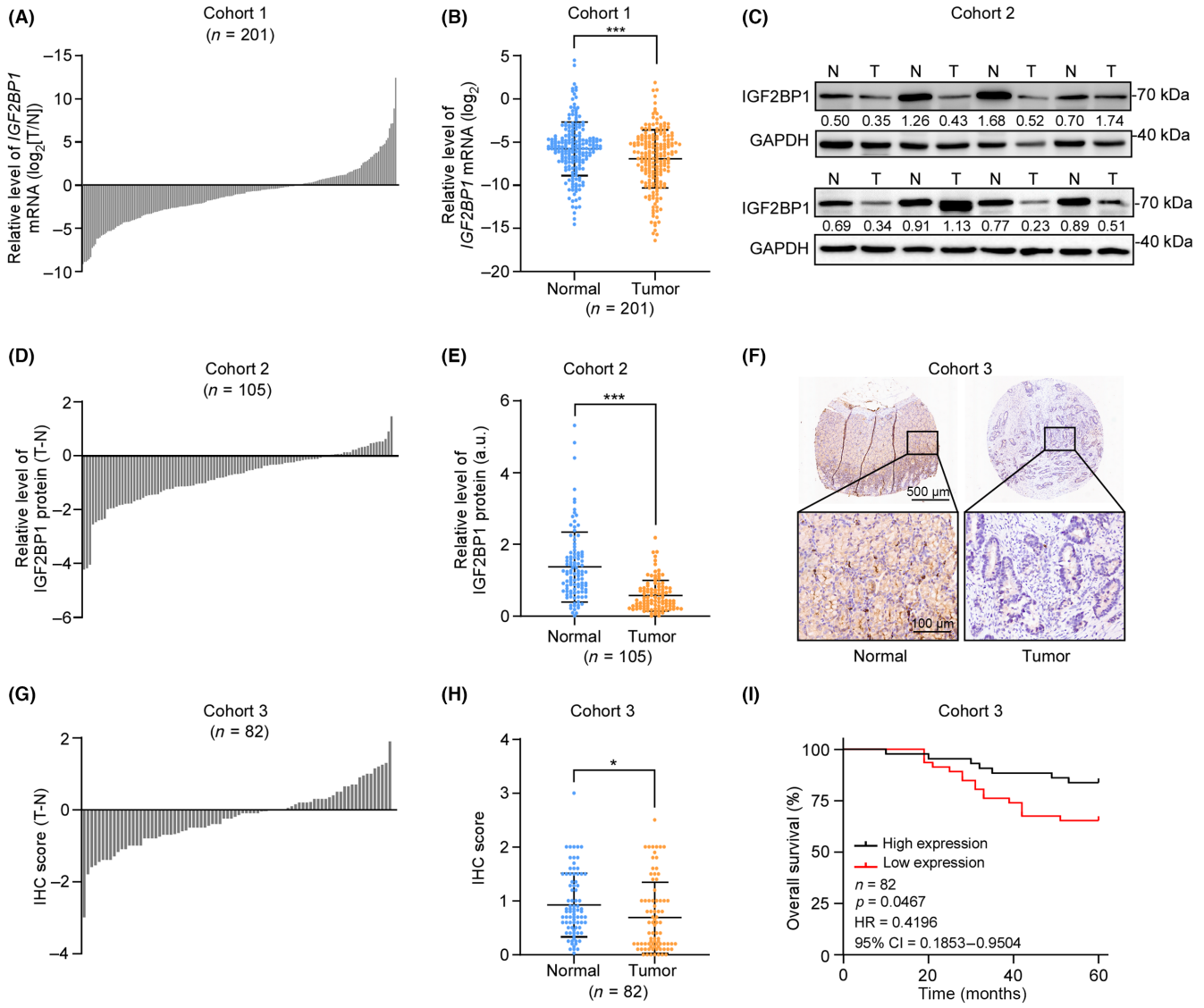

FIGURE 1 Insulin-like growth factor-2 mRNA binding protein 1 (IGF2BP1) levels are significantly downregulated in gastric cancer tissues and negatively associated with poor prognosis. (A, B) Quantitative RT-PCR analyses of *IGF2BP1* mRNA expression in gastric cancer tissues (T) and their adjacent nontumor tissues (N) from cohort I. *GAPDH* served as a loading control. (C–E) Western blot analysis of IGF2BP1 protein in gastric cancer tissues (T) and their adjacent nontumor tissues (N) from cohort 2. (D, E) Quantification analysis of western blotting. GAPDH, loading control. (F–H) Immunohistochemistry (IHC) analysis of gastric cancer tissue array with anti-IGF2BP1 antibody. (F) Representative IHC pictures. (G, H) IHC scores were analyzed. (I) Kaplan–Meier survival curve of IGF2BP1 protein expression in gastric cancer tissues from cohort 3 with best cut-off. Data are shown as mean ± SD. (B, E, H) Paired Student's *t*-test, (I) log-rank test. $^{*}p < 0.05$, $^{***}p < 0.001$. CI, confidence interval; HR, hazard ratio.

lower in AGS cells. Then, we generated WT IGF2BP1 construct to determine the effects of IGF2BP1 overexpression on gastric cancer cell proliferation in AGS cells. The CCK-8 and 2D colony formation assays showed that ectopic expression of IGF2BP1 significantly inhibited cell viability (Figure 2B,C) and reduced the number of 2D colonies formed (Figure 2D,E). Moreover, 3D colony formation assay revealed that exogenous expression of IGF2BP1 also significantly decreased the number and size of 3D colonies (Figure 2F–H).

Meanwhile, we depleted IGF2BP1 in MKN45 cells with two different siRNAs targeting IGF2BP1, and found that IGF2BP1 knockdown resulted in enhanced cell viability (Figure 2I,J) and increased number of 2D colonies (Figure 2K,L). Additionally, we infected MKN45 cells with two lentiviruses carrying shRNAs targeting IGF2BP1 and processed to 3D colony formation experiments. Our results showed an increase in the number and size of 3D colonies in IGF2BP1-depleted cells (Figure 2M–P). Thus, these observations indicate that IGF2BP1 represses the proliferation of gastric cancer cells.

3.3 | IGF2BP1 inhibits gastric cancer cell proliferation in an m^{6}A-dependent manner

It has been reported that mutations in both KH3 and KH4 domains (KH3/4 mutation) or mutations in all KH domains (KH1–4 mutation)

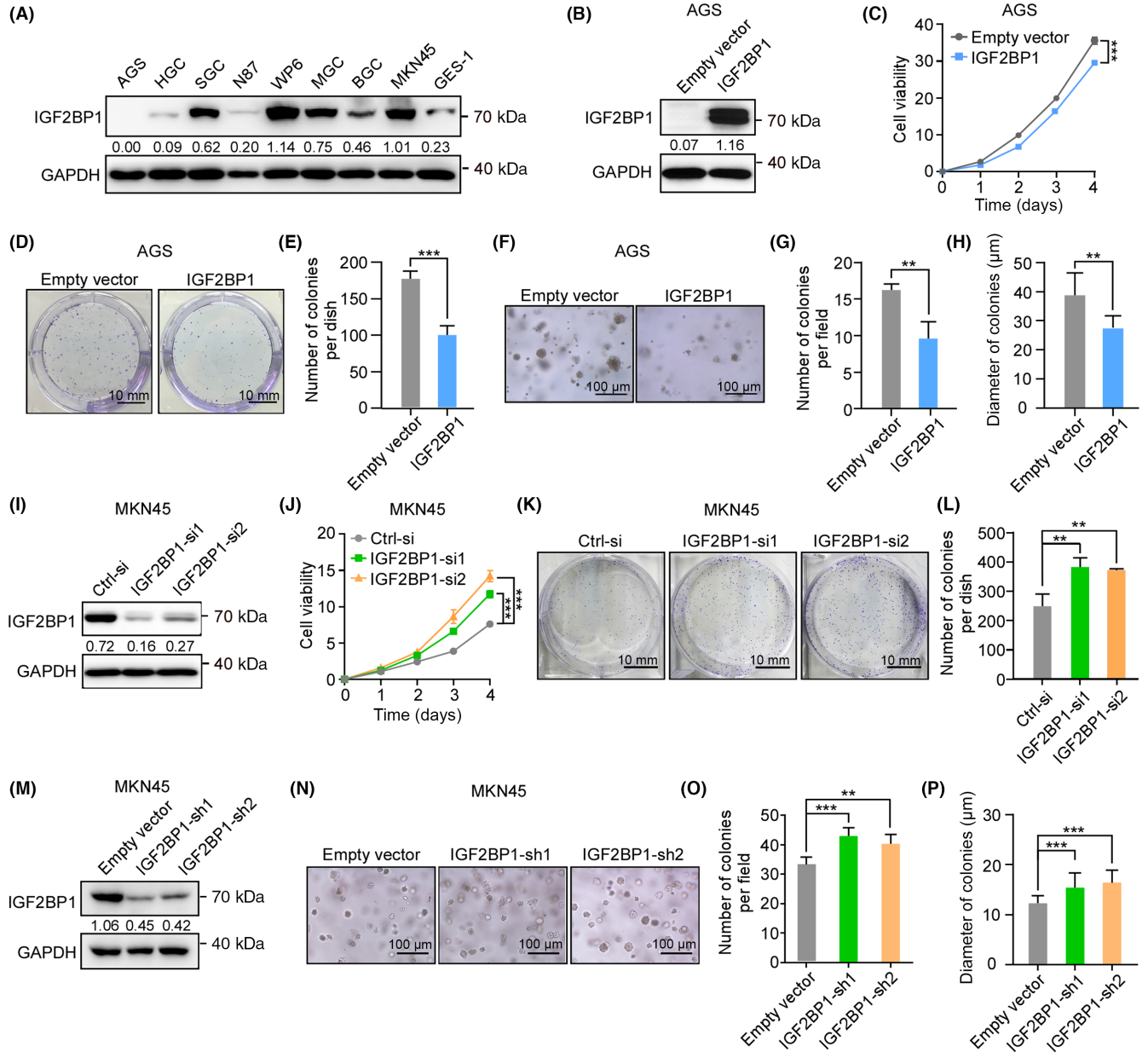

FIGURE 2 Insulin-like growth factor-2 mRNA binding protein 1 (IGF2BP1) suppresses the proliferation of gastric cancer cells. (A) Proteins from the indicated gastric cancer cell lines were subjected to western blot analysis with anti-IGF2BP1 Ab. GAPDH, loading control. (B–H) AGS cells were infected with lentivirus carrying empty pLVX-Puro vector or WT IGF2BP1 for 48 h and applied for western blotting, CCK-8, 2D colony, and 3D colony formation assays. (I–L) MKN45 cells treated with the control siRNA (Ctrl-si) or siRNAs targeting IGF2BP1 for 48 h were subjected to the indicated assays. (M–P) MKN45 cells were infected with lentivirus-based IGF2BP1 shRNAs for 48 h and processed for 3D colony formation assays. (B, I, M) Western blotting of IGF2BP1 protein. (C, J) Cell viability was examined by CCK-8 assays. (D, K) Representative images of 2D colony formation assay. (F, N) Representative images of 3D colony formation assay. (E, G, L, O) Number of colonies was calculated. (H, P) Diameter of colonies was analyzed . Data are expressed as means ± SEM. $^{**}p < 0.01$, $^{***}p < 0.001$; Student's *t*-test.

abolish the m^{6}A recognition and binding capacity of IGF2BP1.[11] To determine whether the role of IGF2BP1 in gastric cancer cell proliferation is dependent on its m^{6}A binding, we constructed IGF2BP1 mutants with mutations in the KH3 and KH4 domains (IGF2BP1-KH3/4) or in the KH1–4 domains (IGF2BP1-KH1-4) (Figure 3A). Exogenous expression of WT IGF2BP1 was able to significantly inhibit the proliferation of AGS cells, while overexpression of IGF2BP1 mutants had no obvious effect (Figure 3B–H). Furthermore, the enhanced proliferation ability of MKN45 cells with IGF2BP1 depletion was significantly overcome by WT IGF2BP1 overexpression, but not by IGF2BP1 KH domain mutants (Figure 3I–P). These data suggest that IGF2BP1 acts as an m^{6}A reader to inhibit gastric cancer cell proliferation.

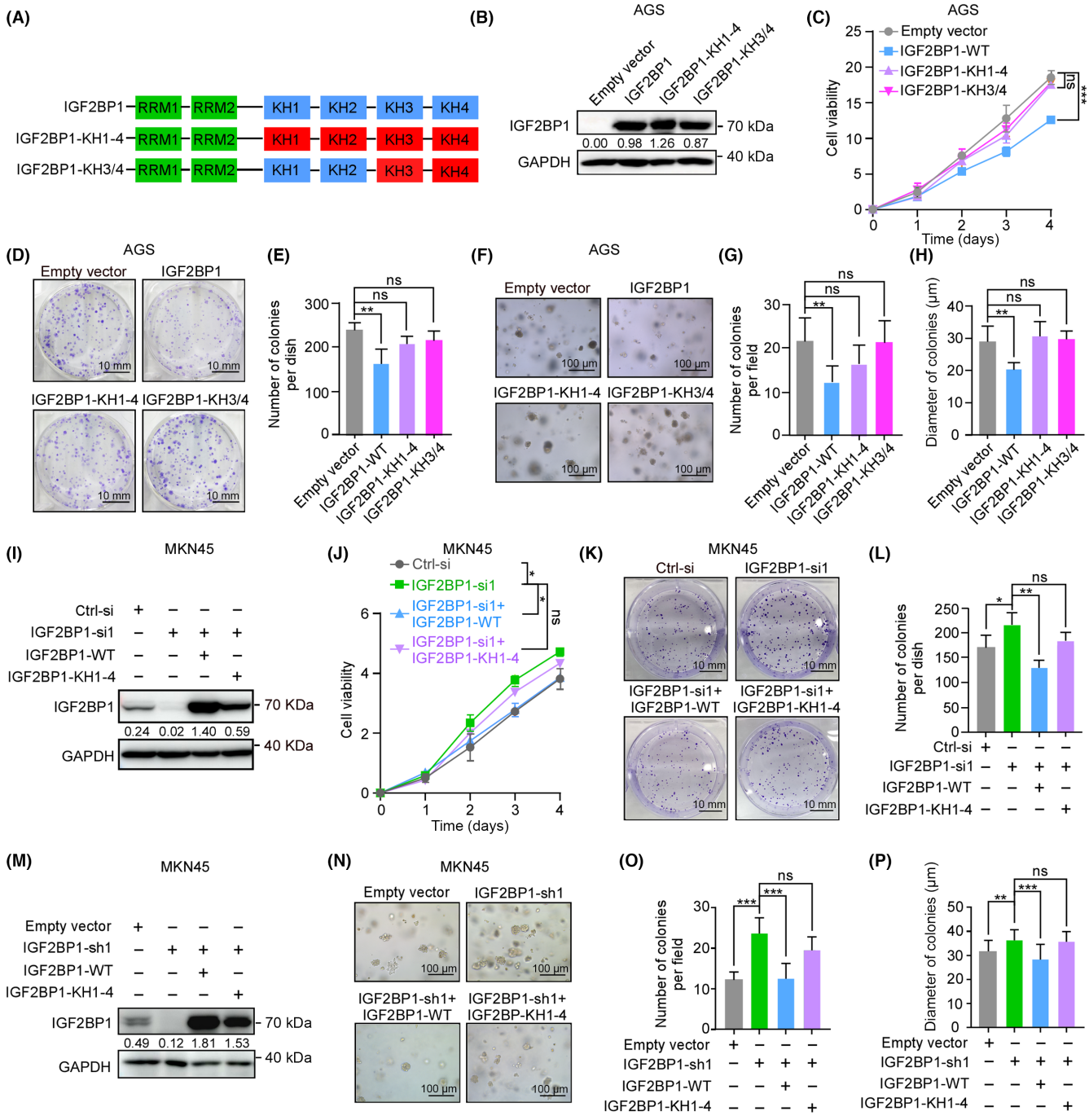

FIGURE 3 Insulin-like growth factor-2 mRNA binding protein 1 (IGF2BP1) inhibits the proliferation of gastric cancer cells through its N^6-methyladenosine (m^6A) recognition domain. (A) Schematic of RNA recognition motif and type I hnRNP K homology (KH) domains within IGF2BP1 proteins. RRM, RNA recognition motif. (B–H) AGS cells were infected with lentivirus carrying empty pLVX-Puro vector, WT IGF2BP1, IGF2BP1-KH1-4, or IGF2BP1-KH3/4 mutants for 48 h and subjected to western blot analysis, CCK-8, 2D colony, and 3D colony formation assays. (I–L) MKN45 cells treated with control siRNA (Ctrl-si) or IGF2BP1 siRNA for 48 h were transfected with WT IGF2BP1 or IGF2BP1-KH1-4 plasmids and applied for the indicated assays. (M–P) MKN45 cells infected with lentivirus-based empty pLKO.1 vectors or IGF2BP1 shRNAs for 48 h were transfected with the indicated plasmids, then subjected to western blot analysis and 3D colony formation assays. (B, I, M) Western blotting of IGF2BP1 protein. (C, J) Cell viability was detected by CCK-8 assays. (D, K) Representative images of 2D colony formation assay. (F, N) Representative images of 3D colony formation assay. (E, G, L, O) Number of colonies was calculated. (H, P) Diameter of colonies was analyzed. GAPDH served as a loading control. Data are expressed as means ± SEM. $^*p < 0.05$; $^{**}p < 0.01$; $^{***}p < 0.001$; Student's *t*-test. ns, not significant.

3.4 | IGF2BP1 represses tumor growth of gastric cancer cells

To examine the effect of IGF2BP1 on gastric cancer cell proliferation in vivo, we first infected MKN45 cells with lentivirus-based shRNA targeting IGF2BP1. Western blots showed that IGF2BP1 was successfully depleted (Figure 4A). Subcutaneous implantation analysis of gastric cancer cells in nude mice revealed that knockdown of IGF2BP1 significantly promoted tumor growth compared with control cells (Figure 4B,C). Moreover, AGS cells were infected with lentiviruses expressing IGF2BP1 to generate gastric cancer cells stably expressing IGF2BP1 (Figure 4D). Exogenous expression of IGF2BP1 significantly inhibited the growth of s.c. xenografted tumors (Figure 4E,F). Therefore, these data indicate that IGF2BP1 could have a tumor-suppressive functions in gastric carcinogenesis.

3.5 | IGF2BP1 impairs gastric cancer cell proliferation by reducing *MYC* expression

As IGF2BP1 influences gastric cancer cell proliferation in an m^{6}A-dependent manner, we undertook m^{6}A-RIP seq and RNA-seq in IGF2BP1-depleted MKN45 cells to explore the potential target transcript mediating the role of IGF2BP1 in gastric cancer cells. Bioinformatic analysis revealed 53 overlapping transcripts acquired from RNA-seq ($|\log_2(\text{fold change})| > 0.6$, $p < 0.01$, $n = 271$) and m^{6}A-RIP seq ($|\log_2(\text{fold change})| > 2$, lgFDR<−5, $n = 1165$) datasets (Figure 5A, Table S3). The TOP10 transcripts (ranked by the "peaks diff. lgFDR" and "peaks lgFDR" values) were further selected for verification (Figure 5B). The m^{6}A-RIP-qPCR and qRT-PCR experiments showed that only *MYC* and *RBM15B* mRNA showed significant changes in both m^{6}A abundance and RNA levels upon IGF2BP1 knockdown (Figure 5C,D), implying that *MYC* and *RBM15B* mRNA may be targets of IGF2BP1 in gastric cancer cells.

To further clarify whether *MYC* or *RBM15B* mediates the role of IGF2BP1 in gastric cancer proliferation, we explored the effect of *MYC* or *RBM15B* knockdown on gastric cancer cell proliferation. Depletion of *MYC* significantly suppressed the proliferative ability of MKN45 cells (Figure S1), whereas *RBM15B* knockdown had no significant effect on MKN45 cell proliferation (Figure S2), suggesting that *MYC*, but not *RBM15B*, could be a downstream target to mediate the function of IGF2BP1 in gastric cancer. To confirm this assumption, we undertook rescue experiments in IGF2BP1-depleted cells by silencing *MYC*. Notably, the enhanced proliferative ability of MKN45 cells with IGF2BP1 depletion was significantly reversed by *MYC* knockdown (Figure 5E–K). Taken together, these data indicate that IGF2BP1 suppresses gastric cancer cell proliferation by reducing *MYC* expression.

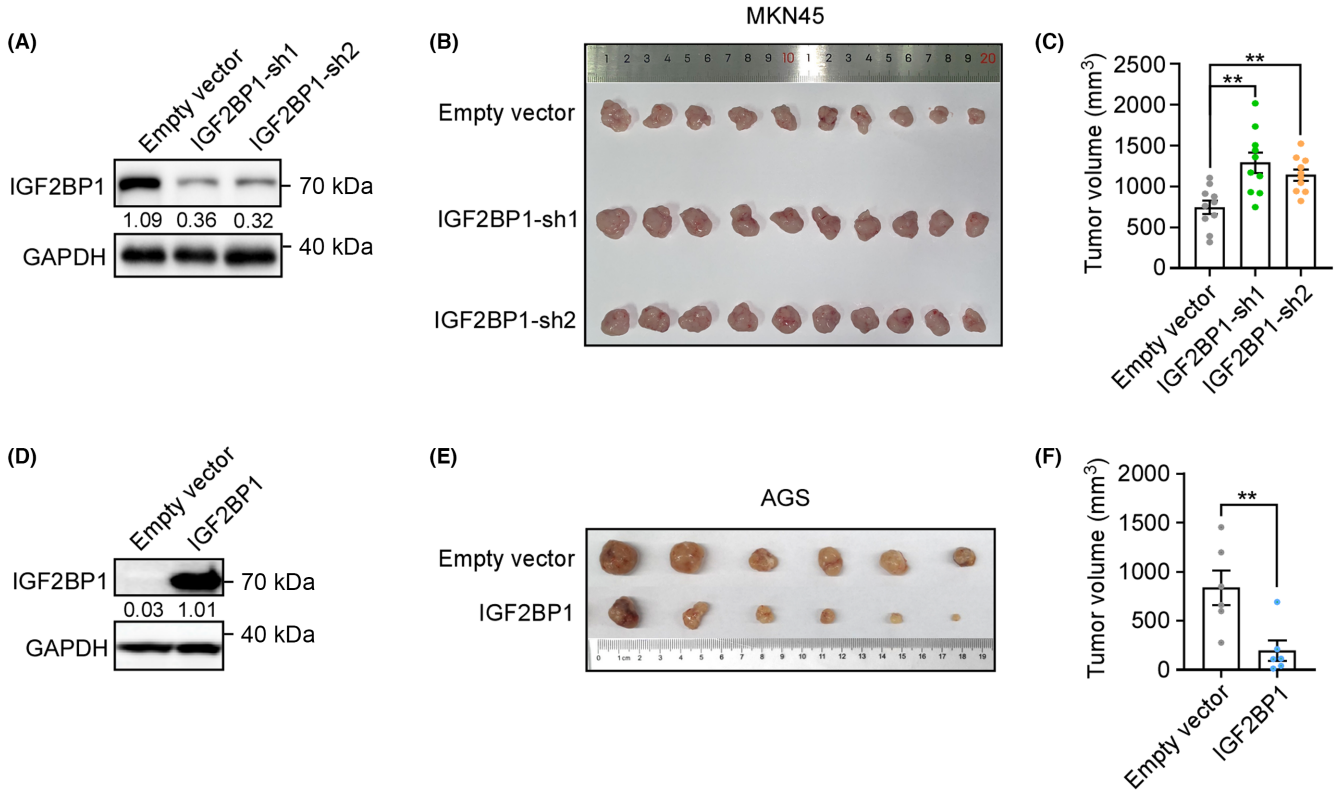

FIGURE 4 Insulin-like growth factor-2 mRNA binding protein 1 (IGF2BP1) suppresses tumor growth of gastric cancer cells. (A–C) MKN45 cells infected with lentivirus-based empty pLKO.1 vectors or IGF2BP1 shRNAs were s.c. injected into BALB/C nude mice. (D–F) AGS cells treated with lentivirus carrying empty pLVX-Puro vector or WT IGF2BP1 were s.c. injected into BALB/C nude mice. (A, D) Western blotting of IGF2BP1 protein from injected cells. (B, E) Subcutaneous tumors. (C, F) Analysis of tumor volume at the end of the experiment. Data are expressed as means ± SEM. $^{**}p < 0.01$; Student's *t*-test.

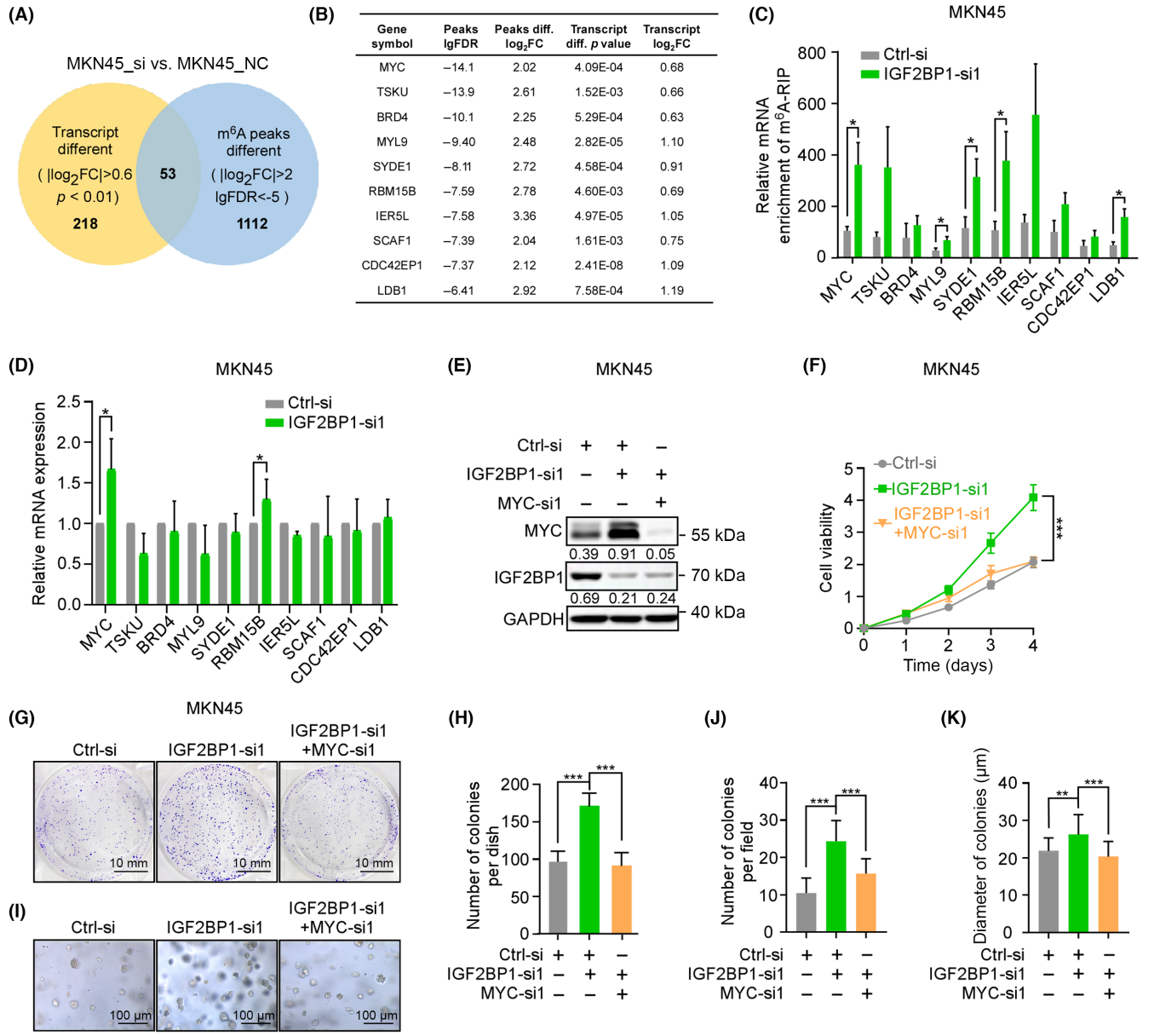

Gene symbol	Peaks lgFDR	Peaks diff. log_2FC	Transcript diff. *p* value	Transcript log_2FC
MYC	−14.1	2.02	4.09E-04	0.68
TSKU	−13.9	2.61	1.52E-03	0.66
BRD4	−10.1	2.25	5.29E-04	0.63
MYL9	−9.40	2.48	2.82E-05	1.10
SYDE1	−8.11	2.72	4.58E-04	0.91
RBM15B	−7.59	2.78	4.60E-03	0.69
IER5L	−7.58	3.36	4.97E-05	1.05
SCAF1	−7.39	2.04	1.61E-03	0.75
CDC42EP1	−7.37	2.12	2.41E-08	1.09
LDB1	−6.41	2.92	7.58E-04	1.19

FIGURE 5 Insulin-like growth factor-2 mRNA binding protein 1 (IGF2BP1) depletion promotes gastric cancer cell proliferation by upregulating MYC expression. (A, B) MKN45 cells treated with control siRNA (NC) or IGF2BP1 siRNA were subjected to N^6-methyladenosine (m^6A)-RNA immunoprecipitation sequencing (RIP seq) and RNA sequencing. (A) Differentially expressed genes with significant changes in m^6A peak abundance in IGF2BP1 depletion cells were analyzed. (B) TOP10 of overlapped genes are listed in the table. (C, D) MKN45 cells treated with control siRNA (Ctrl-si) or IGF2BP1 siRNA were applied for m^6A-RIP-qPCR and quantitative RT-PCR (qRT-PCR). Data are expressed as means ± SD. (E–K) MKN45 cells transfected with the indicated siRNAs were subjected to western blot analysis, CCK-8, 2D colony, and 3D colony formation assays. (E) Western blotting of IGF2BP1 and MYC protein. (F) Cell viability was detected by CCK-8 assay. (G) Representative image of 2D colony formation and (I) 3D colony formation assays. (H, J) Number of colonies was calculated. (K) Diameter of colonies was measured. Data are expressed as means ± SEM. GAPDH served as a control for western blotting and qRT-PCR. $^*p < 0.05$; $^{**}p < 0.01$; $^{***}p < 0.001$; Student's *t*-test. FC, fold change; lgFDR, log_{10}(false discovery rate).

3.6 | IGF2BP1 promotes *MYC* mRNA decay and inhibits its translation

To determine whether the regulation of IGF2BP1 to *MYC* mRNA is associated with m^6A modification, we assessed the mRNA and protein level expression of MYC. Our results revealed that both mRNA and protein expression of MYC were significantly upregulated in IGF2BP1-depleted MKN45 cells (Figure 6A,B). In addition, ectopic expression of WT IGF2BP1, but not IGF2BP1 KH3/4 or KH1-4 mutants, inhibited the MYC expression in AGS cells (Figure 6C,D). Moreover, m^6A-RIP-qPCR assays showed that the enrichment of *MYC* mRNA immunoprecipitated by anti-m^6A Abs was significantly elevated in IGF2BP1-depleted cells compared to that in control cells (Figure 6E). Further RIP experiments revealed that IGF2BP1 protein

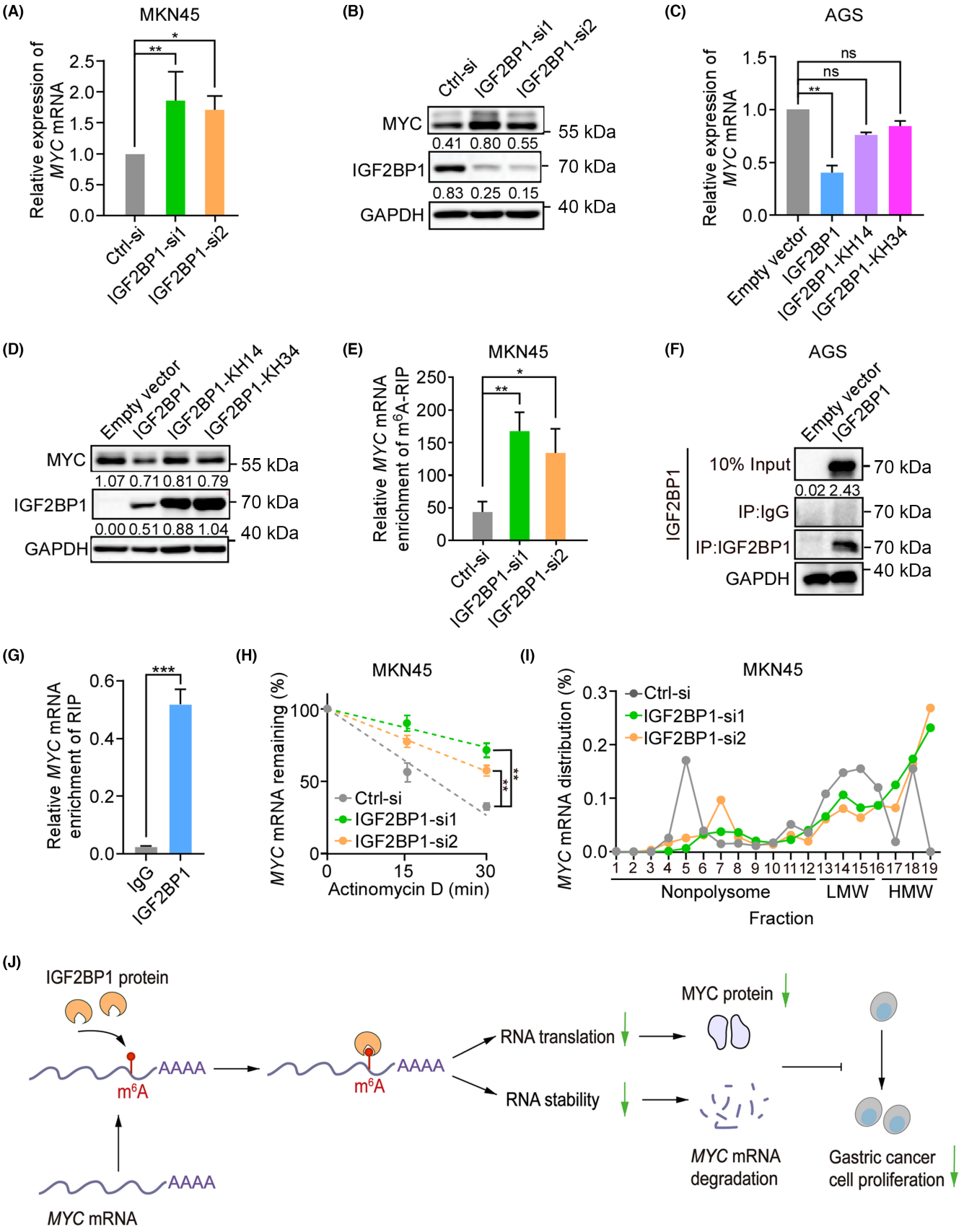
(A)
MKN45
Relative expression of MYC mRNA
Ctrl-si
IGF2BP1-si1
IGF2BP1-si2
(B)
Ctrl-si
IGF2BP1-si1
IGF2BP1-si2
MYC
55 kDa
0.41 0.80 0.55
IGF2BP1
70 kDa
0.83 0.25 0.15
GAPDH
40 kDa
(C)
AGS
Relative expression of MYC mRNA
ns
Empty vector
IGF2BP1
IGF2BP1-KH14
IGF2BP1-KH34
(D)
Empty vector
IGF2BP1
IGF2BP1-KH14
IGF2BP1-KH34
MYC
55 kDa
1.07 0.71 0.81 0.79
IGF2BP1
70 kDa
0.00 0.51 0.88 1.04
GAPDH
40 kDa
(E)
MKN45
Relative MYC mRNA enrichment of m6A-RIP
(F)
AGS
Empty vector
IGF2BP1
IGF2BP1
10% Input
70 kDa
0.02 2.43
IP:IgG
70 kDa
IP:IGF2BP1
70 kDa
GAPDH
40 kDa
(G)
Relative MYC mRNA enrichment of RIP
IgG
IGF2BP1
(H)
MKN45
MYC mRNA remaining (%)
Ctrl-si
IGF2BP1-si1
IGF2BP1-si2
Actinomycin D (min)
(I)
MKN45
MYC mRNA distribution (%)
Ctrl-si
IGF2BP1-si1
IGF2BP1-si2
Nonpolysome
LMW
HMW
Fraction
(J)
IGF2BP1 protein
AAAA
m6A
MYC mRNA
RNA translation
RNA stability
MYC protein
MYC mRNA degradation
Gastric cancer cell proliferation

FIGURE 6 Insulin-like growth factor-2 mRNA binding protein 1 (IGF2BP1) promotes the degradation of *MYC* mRNA and inhibits its translation. (A, B) MKN45 cells treated with control siRNA (Ctrl-si) or IGF2BP1 siRNAs were subjected to quantitative RT-PCR (qRT-PCR) and western blot analysis. (C, D) AGS cells transfected with the indicated plasmids were applied for qRT-PCR and western blotting. (E) MKN45 cells treated with control siRNA or IGF2BP1 siRNAs were subjected to N^6-methyladenosine (m^6A)-RNA immunoprecipitation (RIP)-qPCR assay. m^6A levels of *MYC* mRNA in control and IGF2BP1-depleted cells were measured. (F, G) AGS cells transfected with empty pLVX-Puro vector or WT IGF2BP1 were applied for RIP-qPCR assay. *MYC* mRNA immunoprecipitated by anti-IgG or IGF2BP1 Abs were determined. GAPDH served as a control. Data are expressed as means ± SD. (H) MKN45 cells treated with control siRNA or IGF2BP1 siRNAs were applied for RNA stability assay. Data are expressed as means ± SEM. (I) MKN45 cells treated with control siRNA or IGF2BP1 siRNAs were subjected to polysome profiling analysis. (J) Working model of the regulation of MYC expression by IGF2BP1. $^*p < 0.05$; $^{**}p < 0.01$; $^{***}p < 0.001$; Student's *t*-test. ns, not significant.

was able to interact with *MYC* mRNA (Figure 6F,G). These observations indicate that IGF2BP1 binds to *MYC* mRNA and inhibits the expression of *MYC* mRNA in an m^6A-dependent manner.

Next, we investigated the mechanism by which IGF2BP1 regulates *MYC* mRNA expression by detecting the degradation and translation efficiency of *MYC* mRNA. IGF2BP1-depleted MKN45 cells were treated with actinomycin D for the indicated time periods followed by qRT-PCR. The results showed that the decay rate of *MYC* mRNA was significantly reduced in IGF2BP1-depleted cells (Figure 6H). Additionally, polysome profiling assays revealed that depletion of IGF2BP1 resulted in increased *MYC* mRNA in high molecular weight polysome fractions, indicating higher translation efficiency of *MYC* mRNA (Figure 6I). Collectively, these data suggest that IGF2BP1 facilitates *MYC* mRNA degradation and inhibits its translation efficiency.

4 | DISCUSSION

In this study, we found that the expression of the m^6A reader IGF2BP1 is significantly decreased in gastric cancer tissues and associated with poor prognosis in patients. IGF2BP1 inhibits gastric cancer cell proliferation and tumor growth, indicating a tumor-suppressive role for IGF2BP1 in gastric cancer progression. Mechanistically, IGF2BP1 suppresses the stability and translation efficiency of *MYC* mRNA to hinder the expression of MYC protein through an m^6A-dependent mechanism in gastric cancer cells, consequently resulting in the inhibition of cell proliferation (Figure 6J).

Our analyses of the correlation between IGF2BP1 expression and clinicopathologic features show that lower IGF2BP1 expression is more frequent in gastric cancer tissues with poorer differentiation and lymph node metastasis, suggesting that IGF2BP1 could be involved in the differentiation and metastatic processes of gastric cancer cells. Additionally, we find that lower IGF2BP1 expression is also significantly associated with advanced TNM stages and reduced overall survival time, indicating that the expression level of IGF2BP1 might act as a prognostic predictor for patients with gastric cancer. However, *IGF2BP1* has been previously regarded as an oncogene in some cancers, including non-small-cell lung cancer, hepatocellular carcinoma, and endometrial cancer.[19] These contradictory roles of IGF2BP1 in different cancers could result from the complexity of tumorigenesis. IGF2BP1 may participate in different signaling pathways in different tumors. However, the highly tissue-specific tumor microenvironment might contribute to different cellular responses to IGF2BP1 expression.

Earlier studies have shown that IGF2BP1 stabilizes *MYC* mRNA in several cancer cell lines, such as HCT116 and HepG2. It has been shown that IGF2BP1 binds to and shields the *MYC* coding region instability determinant from endonucleolytic attack, thereby extending its half-life.[20,21] However, our data evidently reveal that IGF2BP1 promotes the degradation and inhibits translation of *MYC* mRNA in gastric cancer cells. These results highlighted that there might be a different mechanism underlying the regulation of *MYC* mRNA by IGF2BP1 in different cancer cells. Further studies are clearly needed to delineate the detailed mechanism underlying the context-dependent effect of IGF2BP1 on *MYC* mRNA.

AUTHOR CONTRIBUTIONS

Ning Ding: Conceptualization; data curation; investigation; methodology; validation; writing – original draft; writing – review and editing. **Guodong Cao:** Data curation; investigation; methodology; resources; validation. **Zhuo Wang:** Data curation; investigation; methodology; validation. **Shengjun Xu:** Conceptualization; project administration; supervision; validation; visualization; writing – review and editing. **Wenwen Chen:** Conceptualization; formal analysis; investigation; methodology; project administration; supervision; validation; writing – original draft; writing – review and editing.

ACKNOWLEDGEMENTS

The authors are grateful to Dr. Sheng Zheng for his excellent technical assistance.

FUNDING INFORMATION

This work was supported by the Natural Science Foundation of Zhejiang Province (LQ22C070003) and China Postdoctoral Science Foundation (2022 M722764).

CONFLICT OF INTEREST STATEMENT

The authors have no conflicts of interest to declare.

DATA AVAILABILITY STATEMENT

All sequencing data that support the findings of this study have been deposited in NCBI's GEO database under accession number GSE243617. Other data in the current study are available from the corresponding authors upon reasonable request.

ETHICS STATEMENT

Approval of the research protocol by an institutional review board: The use of clinical samples was approved by the Ethics Committee of the Second Affiliated Hospital of the Zhejiang University School of Medicine (2022–0927).

Informed consent: N/A.

Registry and the registration no. of the study/trial: N/A.

Animal studies: The mouse studies were approved by the Ethics Committee of the Second Affiliated Hospital of the Zhejiang University School of Medicine (2022–201).

ORCID

Ning Ding https://orcid.org/0000-0001-5726-1840

REFERENCES

1. Sung H, Ferlay J, Siegel RL, et al. Global cancer statistics 2020: GLOBOCAN estimates of incidence and mortality worldwide for 36 cancers in 185 countries. *CA Cancer J Clin*. 2021;71:209-249.
2. Frye M, Harada BT, Behm M, He C. RNA modifications modulate gene expression during development. *Science*. 2018;361(6409):1346-1349.
3. Liu JZ, Yue YN, Han DL, et al. A METTL3-METTL14 complex mediates mammalian nuclear RNA N6-adenosine methylation. *Nat Chem Biol*. 2014;10(2):93-95.
4. Roundtree IA, Evans ME, Pan T, He C. Dynamic RNA modifications in gene expression regulation. *Cell*. 2017;169(7):1187-1200.
5. Jia G, Fu Y, Zhao X, et al. N6-methyladenosine in nuclear RNA is a major substrate of the obesity-associated FTO. *Nat Chem Biol*. 2011;7(12):885-887.
6. Zheng G, Dahl JA, Niu Y, et al. ALKBH5 is a mammalian RNA demethylase that impacts RNA metabolism and mouse fertility. *Mol Cell*. 2013;49(1):18-29.
7. Wang X, Lu ZK, Gomez A, et al. N6-methyladenosine-dependent regulation of messenger RNA stability. *Nature*. 2014;505(7481):117-120.
8. Wang X, Zhao BS, Roundtree IA, et al. N(6)-methyladenosine modulates messenger RNA translation efficiency. *Cell*. 2015;161(6):1388-1399.
9. Xiao W, Adhikari S, Dahal U, et al. Nuclear m(6)a reader YTHDC1 regulates mRNA splicing. *Mol Cell*. 2016;61(4):507-519.
10. Zaccara S, Ries RJ, Jaffrey SR. Reading, writing and erasing mRNA methylation. *Nat Rev Mol Cell Biol*. 2019;20(10):608-624.
11. Huang H, Weng H, Sun W, et al. Recognition of RNA N(6)-methyladenosine by IGF2BP proteins enhances mRNA stability and translation. *Nat Cell Biol*. 2018;20(3):285-295.
12. Korn SM, Ulshöfer CJ, Schneider T, Schlundt A. Structures and target RNA preferences of the RNA-binding protein family of IGF2BPs: an overview. *Structure*. 2021;29(8):787-803.
13. Ramesh-Kumar D, Guil S. The IGF2BP family of RNA binding proteins links epitranscriptomics to cancer. *Semin Cancer Biol*. 2022;86:18-31.
14. Müller S, Bley N, Glaß M, et al. IGF2BP1 enhances an aggressive tumor cell phenotype by impairing miRNA-directed downregulation of oncogenic factors. *Nucleic Acids Res*. 2018;46(12):6285-6303.
15. Gutschner T, Hämmerle M, Pazaitis N, et al. Insulin-like growth factor 2 mRNA-binding protein 1 (IGF2BP1) is an important protumorigenic factor in hepatocellular carcinoma. *Hepatology*. 2014;59(5):1900-1911.
16. Zhuo W, Liu Y, Li S, et al. Long noncoding RNA GMAN, up-regulated in gastric cancer tissues, is associated with metastasis in patients and promotes translation of Ephrin A1 by competitively binding GMAN-AS. *Gastroenterology*. 2019;156(3):676-691.
17. Dominissini D, Moshitch-Moshkovitz S, Salmon-Divon M, Amariglio N, Rechavi G. Transcriptome-wide mapping of N(6)-methyladenosine by m(6)A-seq based on immunocapturing and massively parallel sequencing. *Nat Protoc*. 2013;8(1):176-189.
18. Gandin V, Sikström K, Alain T, et al. Polysome fractionation and analysis of mammalian translatomes on a genome-wide scale. *J Vis Exp*. 2014;87:51455.
19. Huang X, Zhang H, Guo X, Zhu Z, Cai H, Kong X. Insulin-like growth factor 2 mRNA-binding protein 1 (IGF2BP1) in cancer. *J Hematol Oncol*. 2018;11(1):88.
20. Weidensdorfer D, Stöhr N, Baude A, et al. Control of c-myc mRNA stability by IGF2BP1-associated cytoplasmic RNPs. *RNA*. 2019;15(1):104-115.
21. Zhu PP, He F, Hou YX, et al. A novel hypoxic long noncoding RNA KB-1980E6.3 maintains breast cancer stem cell stemness via interacting with IGF2BP1 to facilitate c-Myc mRNA stability. *Oncogene*. 2021;40(9):1609-1627.

SUPPORTING INFORMATION

Additional supporting information can be found online in the Supporting Information section at the end of this article.

How to cite this article: Ding N, Cao G, Wang Z, Xu S, Chen W. Tumor suppressive function of IGF2BP1 in gastric cancer through decreasing MYC. *Cancer Sci*. 2024;115:427-438. doi:10.1111/cas.16047